Dear Franziska Aemisegger,

We greatly appreciate the reviewers' careful reading of our work and their thoughtful, constructive recommendations. We have addressed the vast majority of the comments, and these revisions have substantially improved the manuscript.

Specifically, both reviewers recommended including a quantitative analysis of moisture source regions. This analysis has now been completed and confirms our previous interpretations. Both reviewers also requested a clearer and more detailed explanation of the precision assessment for atmospheric isotope measurements. In response, we have expanded this section and included the code used for the Monte Carlo simulation of calibrated atmospheric water vapor precision. Furthermore, Reviewer #2 encouraged us to strengthen the discussion of terrestrial moisture recycling. We have expanded this discussion to include the roles of entrainment and soil evaporation in shaping the diurnal cycle of d-excess$_V$ and ^{17}O-excess$_V$.

A detailed point-by-point response to all reviewer comments is provided below, together with the corresponding changes in the revised manuscript. Thank you for your time and consideration.

Sincerely,

Claudia Voigt,

on behalf of all co-authors

Author responses to Reviewer #1

Reviewer Comment:

Major comment #1: Measurements of 17O-excess in atmospheric water vapor using Picarro CRDS analyzers are challenging. Even under optimal conditions, averaging for long time is required to discriminate a meaningful signal from instrumental noise. For L2140 analyzers, the typical 1-second Allan deviation is on the order of ~0.1–0.2 ‰ for both δ18O and δ17O, which results into ~100 per meg uncertainty in 17O-excess . Achieving a precision of ~10 per meg therefore generally requires 10–20 minutes of averaging.

These numbers are indicative, as each L2140 analyzer has specific performance. However, the key point is that such averaging reduces uncertainty only if the noise is white. Atmospheric water vapor at canopy scale is unlikely to exhibit white-noise characteristics on ~70 minute timescales due to e.g. turbulence and boundary-layer dynamics. In the presence of autocorrelation or colored noise, time averaging does not automatically reduce uncertainty as √N; instead, Allan deviation typically reaches a plateau or even increases at longer integration times in these conditions.

This limitation likely explains why measurements of 17O-excess in atmospheric water vapor are relatively rare and why cryogenic trapping followed by off-line analysis can still be a solution. In the context of this paper, the effective uncertainty of the reported 17O-excess

values in the present study is likely underestimated, particularly for diurnal variations and vertical gradients between measurement heights that are of similar magnitude to the expected noise level.

I therefore recommend that the authors clarify (i) the noise structure of their vapor measurements, (ii) how the optimal averaging time was determined, and (iii) how effective uncertainty accounting for non-white noise and autocorrelation was estimated. The authors report that precision was determined using a Monte Carlo simulation. It is not clear on which assumptions the simulation is based on. Does the simulation account for uncorrelated noise and ~static signal (such as the one obtained by the A0211 vaporizer?). Or the simulation also accounts for e.g. turbulence noise spectrum?

I believe this is an important point to address, since the 17O-excess variability the authors observe is about the same order of magnitude of the uncertainty. This comment does not apply to the liquid measurement of precipitation, well and spring water.

Author response:

We agree that the isotopic composition of atmospheric water vapor does not follow a white noise signal, but exhibits natural variability driven by turbulence and boundary layer dynamics. To assess how this natural variability influences measurement uncertainty and to determine the best integration interval, we calculated the Allan deviation for 24-hour isotope records obtained during the study period at our study site. In this analysis, measurements from different sampling heights were combined because records longer than 90 min were not available for individual heights. Consequently, the calculated Allan deviation reflects not only temporal variability but also variability associated with vertical isotope gradients. The resulting Allan deviations are therefore likely higher than those derived from measurements at a single height. An example of the Allan deviation for June is shown in Fig. A1 in the revised manuscript version.

Fig. A1 indicates that the optimal integration interval for $\delta^{17}O$, $\delta^{18}O$, $\delta^{2}H$ and d-excess is on the order of a few minutes. For longer integration times, natural variability leads to larger Allan deviations. In contrast, the Allan deviation of ^{17}O-excess reaches a minimum of about 7 per meg at an averaging time of about 1 hour. Based on this result, we selected a 1-hour integration interval for our analysis.

The precision of the raw isotope data was estimated from these Allan deviation plots. A Monte Carlo simulation was performed to estimate the precision of the calibrated water vapor isotope data. Random normally distributed values were generated within the standard deviations of the raw $\delta^{18}O$, $\delta^{2}H$, and ^{17}O-excess values for (i) atmospheric water vapor, (ii) raw and (iii) reference standard measurements, and (iv) the coefficients describing the mixing-ratio dependency functions for $\delta^{17}O$, $\delta^{18}O$, and $\delta^{2}H$ of the two standards. For each randomly generated parameter set, the full calibration procedure described in the main text was applied. The precision of the calibrated atmospheric water vapor isotope data was estimated from the standard deviation of the calibrated value obtained in the Monte Carlo simulation.

To account for the mass-dependent relationship between $\delta^{17}O$ and $\delta^{18}O$, $\delta^{17}O$ was calculated from $\delta^{18}O$ and ^{17}O-excess, and the coefficients of the mixing ratio dependencu function for

$\delta^{17}O$ were generated by applying the same standardized perturbation used for $\delta^{18}O$. Specifically, the generated coefficients for $\delta^{18}O$ wer converted to a z-score relative to heir mean and standard deviation, and these normalized deviations were then scaled and shifted using the $\delta^{17}O$ standard deviation and mean.

In the previous version, the minimum Allan deviations for $\delta^{17}O$, $\delta^{18}O$, $\delta^{2}H$ of raw atmospheric water vapor were mistakenly used instead of the Allan deviations corresponding to the 1-hour averaging interval. Using the corrected values, the simulation results suggest that the standard deviation of the calibrated data is approximately ± 0.2 ‰, ± 0.4 ‰, ± 2.7 ‰ and ± 15 per meg, and ± 4.2 ‰ for $\delta^{17}O$, $\delta^{18}O$, $\delta^{2}H$, ^{17}O excess, and d-excess, respectively. These standard deviations account for measurement uncertainty, uncertainty introduced by calibration, and natural variability over the 1-hour interval.

For comparison, we also performed Monte Carlo simulation using the SD for 2-min intervals, where the Allan deviation of d-excess is minimal (Fig. A1). The standard deviation of the raw $\delta^{18}O_{2min}$, $\delta^{2}H_{2min}$ and d-excess$_{2min}$ are 0.11 ‰, 0.65 ‰ and 0.5 ‰, respectively. Using these values in the simulation yields calibrated precisions over 2-min intervals of 0.12 ‰, 1.2 ‰ and 1.6 ‰, respectively, providing an estimate of the measurement and calibration uncertainty. We then re-calibrated the full atmospheric water vapor isotope record at 2-min intervals and averaged to 1-hour values to match the temporal scale of ^{17}O-excess. The 95th percentiles of the observed range of SD are 0.6‰, 4 ‰ and 1.7 ‰ for $\delta^{18}O$, $\delta^{2}H$ and d-excess, respectively. These values primarily reflect natural variability over the 1hour interval.

Changes in the manuscript:

In the revised manuscript version, we have expanded the corresponding section in the manuscript accordingly. In the appendix, we provide now a figure of the Allan deviations for all isotopic tracers for 24 hours intervals recorded in June 2021 (Fig. A1) and the averages and standard deviations of the coefficients of the mixing ratio dependency functions (Table A2). The MATLAB code used for the Monte Carlo simulation is provided via the data repository ZENODO.

New line 139-156:

The precision of raw isotopic data was estimated from Allan deviation analysis of 24-hour in-situ measurements of atmospheric water vapor at O_3HP in June 2021. While the optimal integration time for $\delta^{17}O$, $\delta^{18}O$, $\delta^{2}H$ and d-excess is on the order of a few minutes, the Allan deviation of ^{17}O-excess reaches a minimum (~7 per meg) at an averaging time of about 1 hour (Fig. A1). To assess the precision of calibrated data, a Monte Carlo simulation was applied following Voigt et al. (2022). In 100 000 iterations, random normally distributed values were generated accounting for the standard deviations of (i) raw $\delta^{18}O_V$, $\delta^{2}H_V$ and ^{17}O-excess$_V$, (ii) the coefficients of the mixing ratio dependency functions of each standard (Table A2) and (iii-iv) the measured and reference values of $\delta^{18}O$, $\delta^{2}H$ and ^{17}O-excess of the two standards. In each iteration, raw atmospheric values were calibrated following the above-described procedure.

The Monte Carlo simulation was run for 2-min integration intervals for $\delta^{18}O$, $\delta^{2}H$ and d-excess and for 1-hour integration intervals for ^{17}O-excess. Over 2-min intervals, the raw Allan deviations were 0.11 ‰ for $\delta^{18}O$, 0.65 ‰ for $\delta^{2}H$ and 0.5 ‰ for d-excess, yielding simulated calibrated standard deviations of calibrated 2-min mean values of 0.12 ‰, 1.2 ‰ and 1.6 ‰, respectively. Over 1-hour intervals, the raw Allan deviations were 0.2 ‰ for $\delta^{17}O$, 0.4 ‰ for $\delta^{18}O$, 2.5 ‰ for $\delta^{2}H$, 7 per meg for ^{17}O-excess and 1.6 ‰ for d-excess, yielding simulated standard deviations of calibrated 1-hour mean values of approximately ± 0.2 ‰, ± 0.4 ‰, ± 2.7 ‰ and ± 15 per meg, and ± 4.2 ‰ for $\delta^{17}O$, $\delta^{18}O$, $\delta^{2}H$, ^{17}O-excess, and d-excess, respectively. For consistency, all isotopic tracers were integrated over 1 hour, which also determined the frequency of alternation between measurement heights. This is limited by the resolution achievable for ^{17}O-excess. The simulated standard deviations account for both the measurement precision and the natural variability in the isotopic composition of atmospheric water vapor over the integration interval.

Table A2: Means (AV) and standard deviations (SD) of coefficients of mixing ratio dependency functions for $\delta^{17}O$, $\delta^{18}O$ and $\delta^{2}H$ of the three used standards (ICE: $\delta^{17}O$ = -14.2404 ‰, $\delta^{18}O$ = -26.8485 ‰, $\delta^{2}H$ = -203.76 ‰; NOC: $\delta^{17}O$ = -8.9619 ‰, $\delta^{18}O$ = -16.9109‰, $\delta^{2}H$ = -125.69‰;, TAP: $\delta^{17}O$ = -4.5397 ‰, $\delta^{18}O$ = -8.6382 ‰, $\delta^{2}H$ = -59.24‰). The mixing ratio dependency functions have the form f(x) = a/x+bx+c and are determined relative to a water mixing ratio of 10000 ppmv.

Coefficient	$\delta^{17}O$		$\delta^{18}O$		$\delta^{2}H$	
	AV	SD	AV	SD	AV	SD
ICE						
a	9.37E+02	7.41E+01	1.12E+03	1.01E+02	8.89E+03	4.23E+02
b	3.46E-06	4.72E-07	1.01E-05	8.32E-07	1.12E-05	4.66E-06
c	-1.26E-01	1.37E-02	-2.15E-01	2.16E-02	-1.01E+00	1.15E-01
NOC						
a	6.77E+02	5.60E+01	6.67E+02	9.08E+01	5.27E+03	6.72E+02
b	3.00E-06	7.07E-07	9.44E-06	1.10E-06	1.47E-05	5.94E-06
c	-9.84E-02	1.53E-02	-1.64E-01	2.46E-02	-6.42E-01	1.65E-01
TAP						
a	2.95E+02	9.14E+01	-2.68E+01	1.22E+02	1.62E+02	5.79E+02
b	3.75E-06	6.22E-07	1.05E-05	9.79E-07	1.88E-05	6.98E-06
c	-6.54E-02	1.85E-02	-1.00E-01	2.60E-02	-2.05E-01	1.61E-01

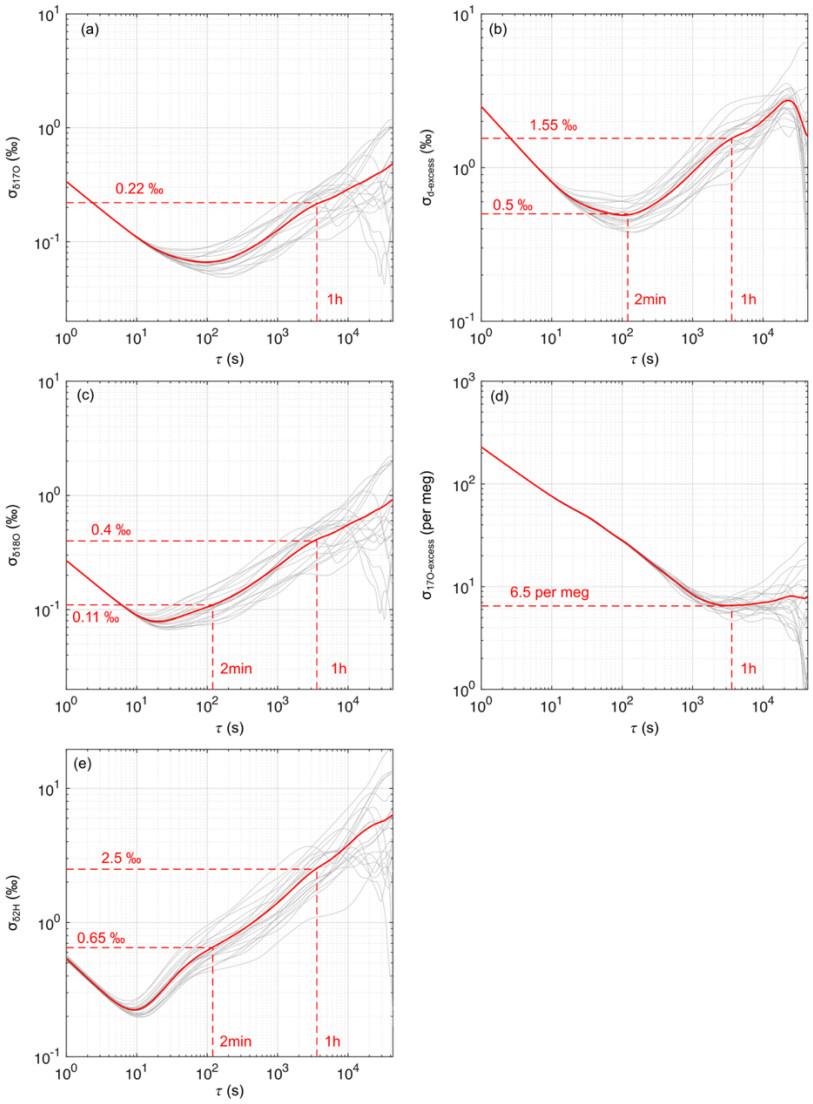

Fig. A1: Allan deviations σ for (a) $\delta^{17}O$, (c) $\delta^{18}O$, (e) $\delta^{2}H$, (b) d-excess and (d) ^{17}O-excess for 24-hour records of atmospheric water vapor at O_3HP gathered between June 1, 2021 and June 30, 2021. The red solid curve illustrates the mean Allan deviations. Dashed lines and associated numbers indicate the Allan deviation for 1 hour and 2 min averaging time, respectively.

Reviewer Comment:

Major comment #2: The authors report water vapor observations using a multiple-inlet system (0.4 m, 1.5 m, 3.5 m, and 12.5 m). However, several key aspects of the sampling configuration are insufficiently described. In particular, the total length of the inlet lines is not stated, and it is not clear whether the individual lines are flushed continuously when not connected to the Picarro via the port distribution manifold. It is also unclear whether the analyzer is connected directly to the inlet distribution manifold or whether an intermediate volume is present (e.g. a buffer or the A0211 vaporizer). Moreover, the reported analyzer flow rate (~0.4 mL/min) is low for such analyzers. My concern is that the combination of potentially unflushed inlet lines and low analyzer flow rates have impact on residence time and memory effects within the sampling system, resulting into signal smoothing and carryover between successive inlets. This

is especialy true when switching between heights characterised by different humidity and isotopic composition. With the information reported by the authors, it is difficult to assess whether the (lack of) observed variability between inlets reflect true atmospheric variability or are partly influenced by sampling-system artefacts. A long-term averaging (e.g. daily or even seasonal) might also have flattened any difference in isotopic composition of water vapor between the inlets at different heights. I recommend that the authors provide a more detailed description of the inlet configuration and flow scheme, e.g. with a diagram, and, if possible, include quantitative tests or estimates of memory effects associated with inlet switching.

Author response:

From bottom to top, the inlet lines were approximately 11.5 m, 15 m, 20 m, and 32 m long. Each line was continuously flushed with a flow rate of 5 L min^{-1}. The port distribution manifold is connected to the vaporizer, which is coupled to the analyzer. The instrument subsampled the inlet lines with a flow rate of 35 mL min^{-1}. We believe that residence times and the memory effect is minimized by the high flush rate. The residence time was less than 20s for the longest tube. However, we discarded the first 10 min of each line measurement to minimize any memory effect.

Changes in the manuscript:

We added this information in the revised manuscript version. In addition, we provide a figure illustrating the experimental setup.

New Line 95-110:

Figure 1 illustrates the experimental setup for in-situ isotope monitoring of atmospheric water vapor. The inlets of four 1/4-inch wide PFA tubes (PFA-T4-062-100, Swagelok, Ohio, US) were positioned at 0.4 m above the grass plot, and at 1.5 m, 3.5 m, and 12.5 m above ground level (agl) – below, within and above the downy oak forest canopy, respectively. From bottom to top, the tubes were approximately of 11.5 m, 15 m, 20 m, and 32 m length. The tubes were continuously pumped at a flow rate of ~5 L min^{-1} using oil-free diaphragm pumps. Along the entire length, the tubing was insulated and heated to 40–50°C using self-regulating heat wire to prevent condensation. A funnel covered by a net was placed at each inlet for protection from rain and suction of insects and large aerosol particles. A split of each line was passed to a 16-Port Distribution Manifold (A0311; Picarro Inc., California, USA) coupled to a high-precision vaporizer (A0211, Picarro Inc., California, USA) and a CRDS (L2140-i; Picarro Inc., California, USA). The instrument was installed in an air-conditioned building on the experimental site and was operated in ^{17}O Dual Liquid/Vapor mode. It subsampled air from a selected tube with a flow rate of about 35 mL min^{-1} for 70 minutes before switching to the next tube. During data processing, the first 10 minutes of each line measurement were discarded to minimize memory effects, and the subsequent 60 minutes were averaged. Such long integration times were necessary to achieve high precision in ^{17}O-excess (see below). From January to May 2021, measurements were alternated between the two tubes positioned at 0.4 m above the grass plot and 12.5 m above the forest canopy, resulting in 9–10 measurements per height and

day. From June to December 2021, measurements were alternated between all four heights, resulting in 4–5 measurements per height and day.

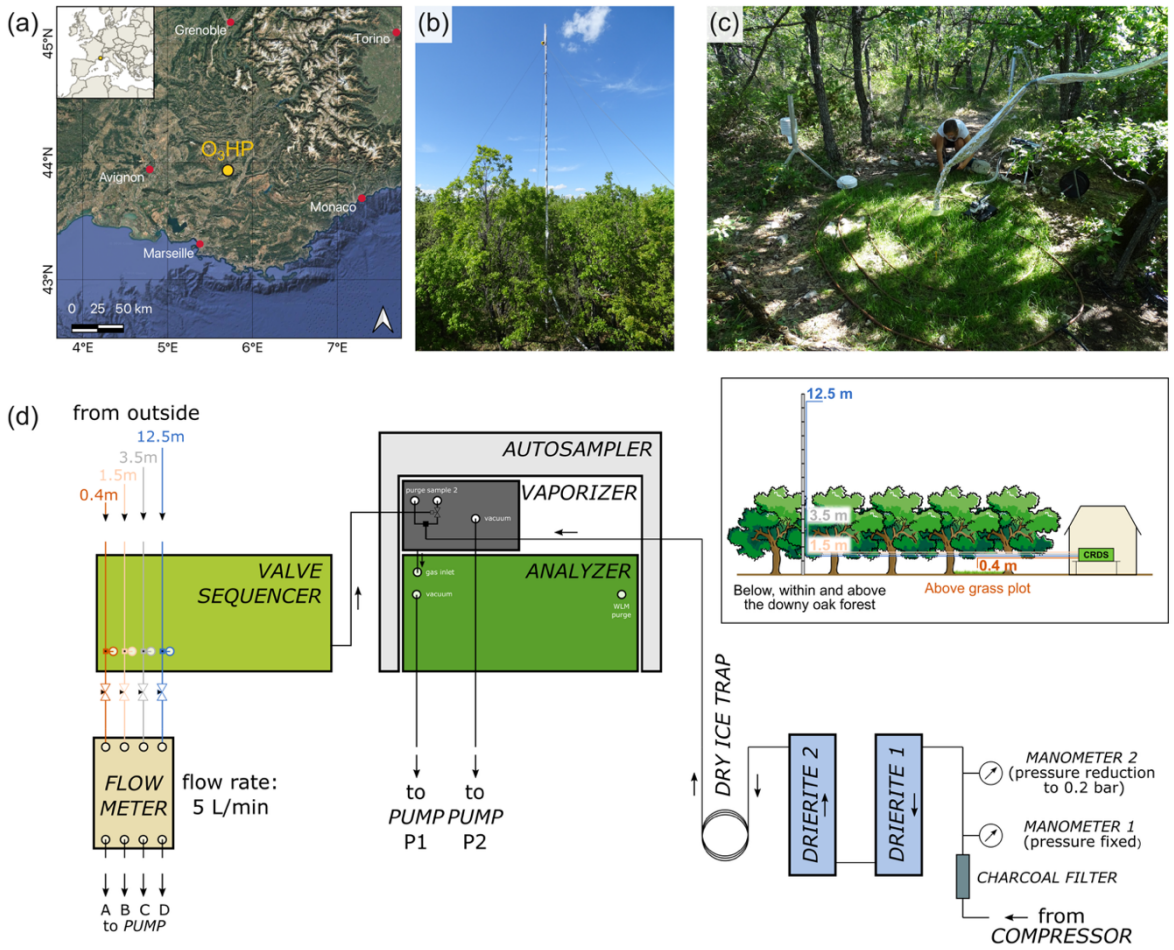

Figure 1: (a) Location of the study site O_3HP. (Map: Google ©2026, Data: SIO, NOAA, U.S. Navy, NGA, GEBCO, Image: Landsat / Copernicus), (b) Mast installed within the downy oak forest canopy, equipped with intake lines for continuous atmospheric water vapor isotope sampling. (Photo: C. Voigt). (c) Grass plot in the forest understory instrumented with micro-climate and atmospheric isotope measurement systems (Photo: A. Alexandre). (d) Schematic illustration of the experimental setup. The solenoid valve behind the vaporizer allowed switching between the valve sequencer used for atmospheric water vapor measurements and the dry air stream provided by the combination of compressed air, drierite columns and the dry ice trap used for weekly calibrations. See text for detailed description.

Reviewer Comment:

Major comment #3: The statistical analysis of air-parcel origins based on back-trajectory frequency does not directly identify moisture sources of precipitation or boundary-layer water vapor origin. In particular, in Section 3.6 (lines 315–320), the attribution of moisture sources remains qualitative, as the analysis considers only the geographic origin of air masses and not the actual moisture exchange of air parcels with the ocean surface (evaporation) or land (evapotranspiration).

This distinction is important because air-mass origin does not necessarily correspond to moisture source, strongly limiting boundary layer water vapor mass-balance

calculation/speculations. During atmospheric transport, water vapor undergo several processes, to mention a few: condensation, re-evaporation, mixing, local evapotranspiration, etc. All of these processes substantially modify the isotopic composition of water vapor. Consequently, caution is required when attributing isotopic signatures to specific moisture sources based solely on back trajectories, particularly for δ18O and δD, whose variability is influenced by several factors such as local temperature and convective activity. In this context, d-excess and likely 17O-excess (as suggested by the manuscript itself) represents a more robust parameter for investigating moisture source conditions.

A more statistically and physically consistent approach would be to combine back trajectories with isotopic observations at the O3HP site, for example using concentration weighted trajectories (implemented in the HYSPLIT framework employed by the authors) which have proven effective in previous studies in the Mediterranean region (e.g. Salamalikis et al., 2015). Another option would be to use a Lagrangian moisture diagnostics that explicitly identify moisture uptake along trajectories (e.g. following Sodemann et al., 2008, as mentioned by the authors in the conclusion). The latter would provide a more rigorous basis for source attribution and mass-balance. Such approach have been successfully applied to disentangle the drivers of water vapor d-excess variability in continental boundary layers (e.g. Aemisegger et al., 2014).

At present, the message conveyed in lines 321–329 is unclear. The interpretation would benefit from rephrasing and acknowledging the limitations of the source attribution method used in this study. A similar caution applies to discussion section 4.1.

Finally, given the proximity of the study site to the Mediterranean Sea, one might also expect a stronger influence from the western Mediterranean and central Europe. The seasonal source decomposition presented by Sodemann and Zubler (2010; their Fig. 8) could serve as a useful reference framework for contextualizing the results (although the latter paper is focused on precipitation only).

The authors should clarify the distinction between air-mass pathways and moisture sources, and edit the interpretation accordingly.

Author response:

We implemented now a Lagrangian moisture source diagnostic following Sodemann et al. (2008). Subsequently, we applied a modified Concentration Weighted Trajectory (CWT) approach after Salamalikis et al. (2015). In addition to the initial author response, we now increased the grid size to 1°x1°. We also used another shapefile to better mask land areas.

Changes in the manuscript:

We implemented the quantitative moisture source analysis in the methods section:

New line 211-235:

Moisture uptake zones were quantified using a Lagrangian moisture source diagnostic following Sodemann et al. (2008). Along each backward trajectory, positive increments in specific humidity ($\Delta q > 0$) calculated at 6-hour intervals were interpreted as moisture uptake

from the underlying surface. Each uptake location was assigned to the midpoint of the corresponding trajectory segment. Only uptake events exceeding 0.2 g kg^{-1} and occurring below 1.5 times the planetary boundary layer height were considered in order to reduce the influence of numerical noise and restrict moisture contributions to boundary-layer exchange processes. Each uptake event was weighted by its relative contribution to the final specific humidity at the study site. If a decrease in specific humidity ($\Delta q < 0$), interpreted as precipitation loss, occurred downstream of one or more uptake events, the contributions of the preceding uptakes were proportionally reduced to account for moisture removal. This procedure yields, for each trajectory, the fractional contribution of a grid cell to q at the study site.

In order to assess the potential relation between the isotopic composition of atmospheric water vapor at the study site and its oceanic moisture source region, we applied a modified Concentration Weighted Trajectory (CWT) approach. A spatial grid of 1° × 1° resolution was defined over the study domain. Instead of weighting the isotopic composition measured at the study site by the residence time in each grid cell, as done by Salamalikis et al. (2015), we weighted it by the previously derived fractional moisture contribution $\tau_{(ij)k}$ of the corresponding hourly trajectory. The isotopic signature assigned to each grid cell (i,j) was computed as:

$$C_{ij} = \frac{\sum_{k=1}^{N} \tau_{ijk} C_k}{\sum_{k=1}^{N} \tau_{ijk}} \quad (7)$$

where C_k is the isotopic composition ($\delta^{18}O$, d-excess, or ^{17}O-excess) measured upon arrival of trajectory k at the study site, and τ_{ijk} is the fractional moisture contribution of grid cell (i,j) to trajectory k. Thus, C_{ij} represents the moisture-contribution-weighted isotopic composition associated with evaporation from grid cell (i,j). For precipitation, all air mass back-trajectories of hours during which rain was detected on-site were compiled and weighted by rainfall amount.

For regional interpretation, we aggregated grid cells into eight predefined source regions after Sodemann and Zuber (2010): NW = Northwest North Atlantic, NE = Northeast North Atlantic, SW = Southwest North Atlantic, SE = Southeast North Atlantic, A = Arctic and Nordic Seas, CE = Central Europe, MW = Western Mediterranean, ME = Eastern Mediterranean. To focus on oceanic moisture sources, only grid cells located over ocean surfaces were considered. Continental areas were masked using the GLDAS Land/Sea Mask Dataset at 1º resolution (NASA/GES DISC., 2026).

We updated the results (Section 3.6) using the new predefined source regions. For prediction of the isotopic composition of water vapor evaporated from the ocean, we focussed only on the major moisture sources NE North Atlantic, SE North Atlantic and the Western Mediterranean.

New Line 384-400:

The moisture source contributions for atmospheric water vapor and precipitation are illustrated in Figure C1 and C2. For atmospheric water vapor, the NE North Atlantic (33%) and the Western Mediterranean (29%) are the dominated moisture sources for our study site (Table C1). For precipitation, most of the moisture is derived from the Western Mediterranean (41%), followed by the NE North Atlantic (25%) and the SE North Atlantic (18%) (Table C2). Changes in the relative contributions of each moisture source over the year are illustrated in Figure C3 and C4 for atmospheric water vapor and precipitation, respectively.

The isotopic compositions of atmospheric water vapor and precipitation clustered by moisture sources were generally similar (Table C1 and C2). In particular, d-excess and ^{17}O-excess of atmospheric water vapor or precipitation coming from the North Atlantic sectors and the Western Mediterranean were not significantly different.

We also compared the monthly average isotopic composition of atmospheric water vapor observed at O_3HP with those estimated above the four oceanic moisture sources (Fig. 6). The latter shows seasonal isotope variability which co-varies with SST and RH_{SST}. Interestingly, from July to December, RH_{SST} over the Mediterranean Sea is systematically lower than over the NE North Atlantic but does not differ from RH_{SST} over the SE North Atlantic. For all sources, $d^{18}O_V$ is higher and d-excess$_V$ and ^{17}O-excess$_V$ are lower in summer than in winter. A similar seasonal trend is evident in the isotopic composition of the water vapor observed at O_3HP (Fig. 6). However, the $\delta^{18}O_V$ values at O_3HP were 3–11 ‰ lower than those estimated for the ocean sources. In contrast, the d-excess$_V$ at O_3HP was of the same order of magnitude as that over the ocean sources, while the observed ^{17}O-excess$_V$ was slightly higher (by 11 ± 5 per meg).

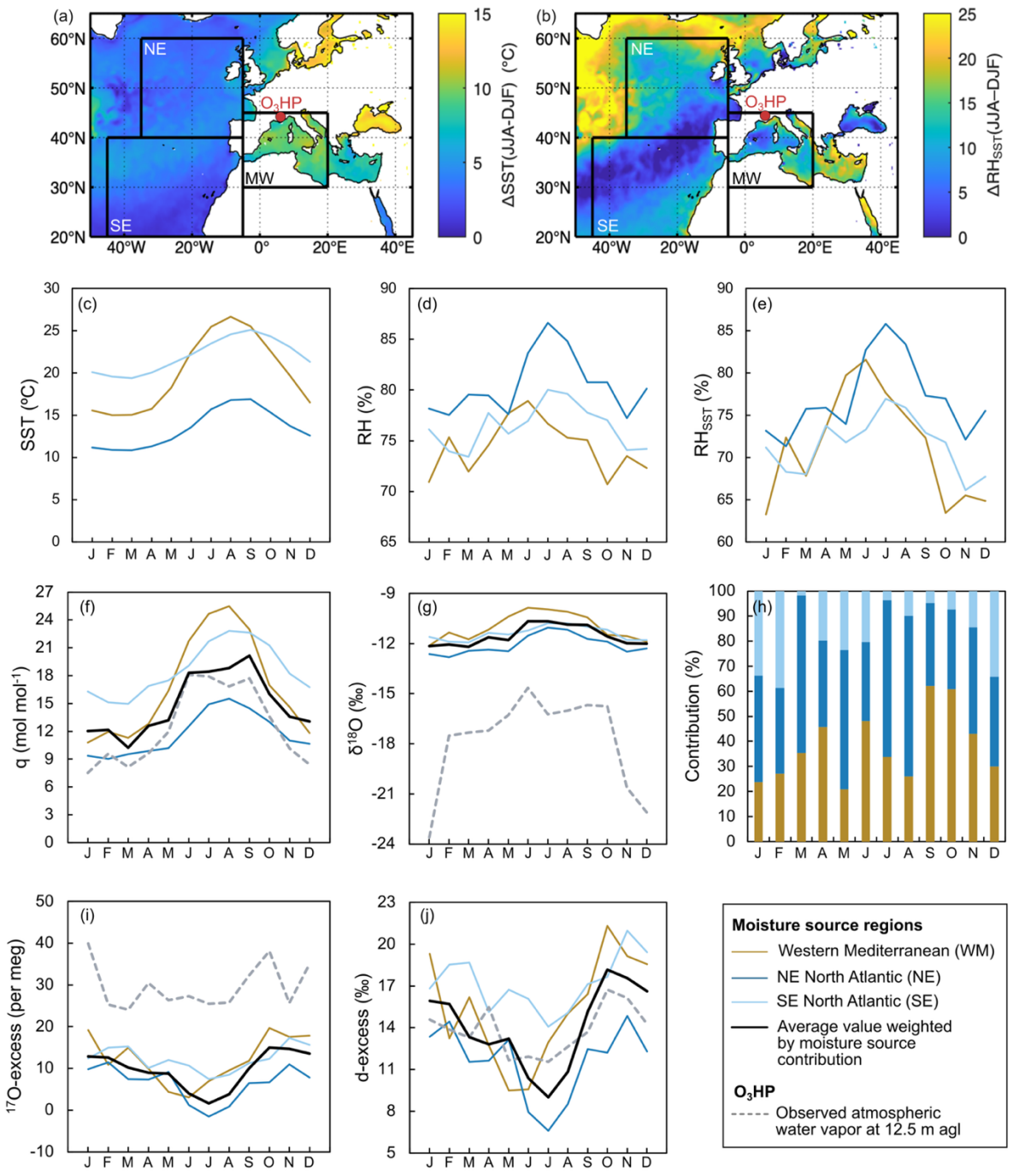

Figure 6: Seasonal and monthly variation in the isotope composition of atmospheric water vapor measured at O_3HP compared with climate parameters and isotope composition of atmospheric water vapor at the three main oceanic moisture sources. (a)-(b) Spatial variability of the difference between summer (JJA) and winter (DJF) sea surface temperature (SST) and relative humidity normalized to SST (RH_{SST}) in 2021. Data derived from ERA5 Reanalysis (Hersbach et al., 2020). The red circle indicates the location of the study site. (c)-(e) Monthly average SST, relative humidity above the ocean (RH) and RH_{SST} obtained from the ERA5 reanalysis dataset (Hersbach et al., 2020) for 2021. (f)-(j) Monthly average of atmospheric water mixing ratio (χ), relative contribution of the three moisture sources obtained from Lagrangian moisture source diagnostic (Sect. 3.6), $\delta^{18}O_V$, d-excess$_V$ and ^{17}O-excess$_V$ measured at O_3HP at 12.5 m agl (dashed line) and estimated above the three main oceanic moisture sources (solid lines). See Sect. 2.5 for more details on how the isotopic composition of water vapor over each moisture source is estimated.

We revised the discussion (Section 4.1) on the influence of moisture sources accordingly.

New Line 440-459:

4.1 Evaporative conditions at the oceanic moisture sources

The three principle oceanic moisture sources show lower RH_{SST} during winter than in summer, resulting in stronger kinetic fractionation during evaporation from the ocean and higher d-excess$_V$ and ^{17}O-excess$_V$ in the evaporated water vapor in winter than in summer (Fig. 6). This seasonal change predicted for water vapor over the oceanic moisture sources is also visible in the d-excess$_V$ measured at O_3HP and to a lesser extent in the ^{17}O-excess$_V$. This consistency suggests that seasonal changes in evaporative conditions at the oceanic moisture sources contribute to seasonal changes in d-excess$_V$ and ^{17}O-excess$_V$ at the study site. This is in agreement with previous interpretations of the triple oxygen isotopic composition of water vapor and precipitation (Affolter et al., 2015; Landais et al., 2012; Liotta et al., 2008; Merlivat & Jouzel, 1979; Pfahl & Sodemann, 2014; Tian et al., 2018; Uechi & Uemura, 2019). However, with regard to $\delta^{18}O_V$, seasonal changes in the evaporative conditions at the oceanic moisture sources are limited to 1.5 ‰ and cannot explain the ~7 ‰ seasonal variations observed at the study site. This indicates that $\delta^{18}O_V$ is likely modified by further fractionation processes.

In previous studies, evaporative conditions at the moisture sources were invoked to explain d-excess$_P$ in precipitation from the Western Mediterranean (~14 ‰) to be higher than in precipitation from the NE North Atlantic (~10 ‰) (Casellas et al., 2019; Celle-Jeanton et al., 2001; Cruz-San Julian et al., 1992; Delattre et al., 2015; Natali et al., 2021). Theoretical predictions indeed show that d-excess$_V$ over NE North Atlantic is about 3.7 ‰ lower than over Western Mediterranean due to higher RH_{SST} (Fig. 6). Similarly, ^{17}O-excess of water vapor evaporated from the Western Mediterranean is predicted to be ~ 6 per meg higher than from the NE North Atlantic, although the magnitude remains within measurement precision. However, d-excess and ^{17}O-excess measured in atmospheric water vapor and precipitation at O_3HP grouped by their primary moisture source (NE North Atlantic vs. Mediterranean) were not significantly different. Several factors may have contributed to diminish the isotopic contrast between these source regions, including frequent mixing of moisture from multiple sources, local orographic and boundary-layer dynamics or moisture recycling during atmospheric transport (Aemisegger et al., 2014; Natali et al., 2022).

We added the results of the moisture source analysis in the appendix:

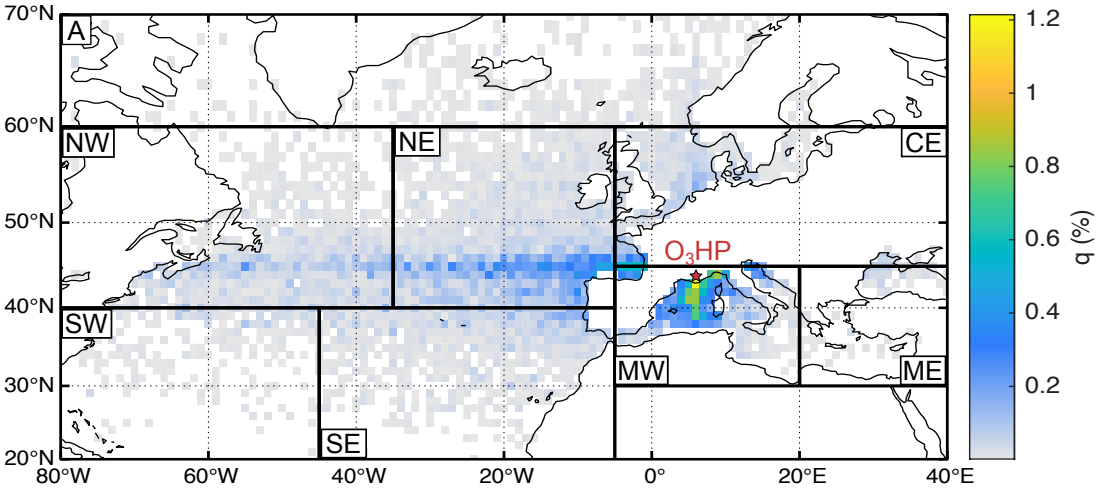

Figure C1: Annual mean oceanic moisture source contributions to atmospheric water vapor at O_3HP. Shading: Relative contribution of evaporation from respective grid cell to the final specific humidity of each trajectory.

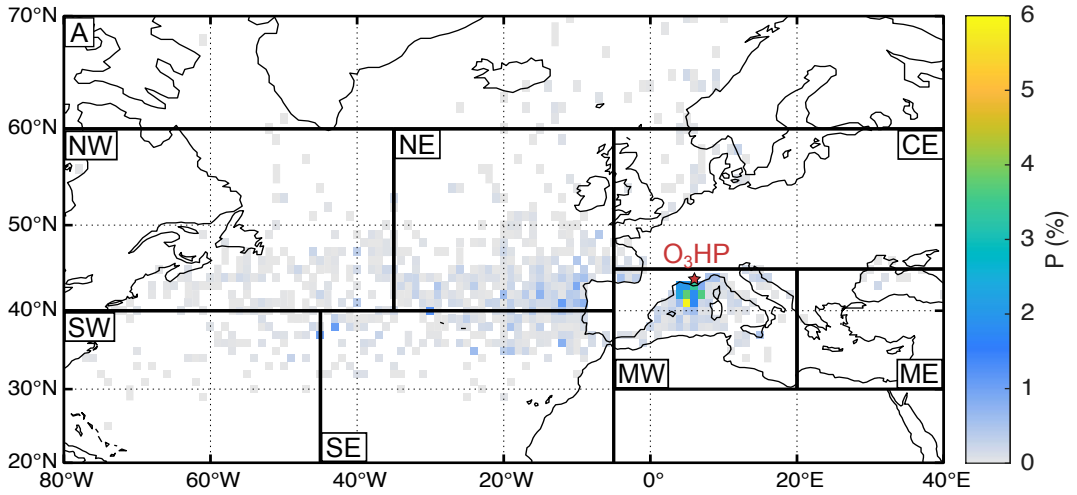

Figure C2: Annual mean oceanic moisture source contributions to precipitation at O_3HP. Shading: Relative contribution of evaporation from respective grid cell to diagnosed precipitation at O_3HP.

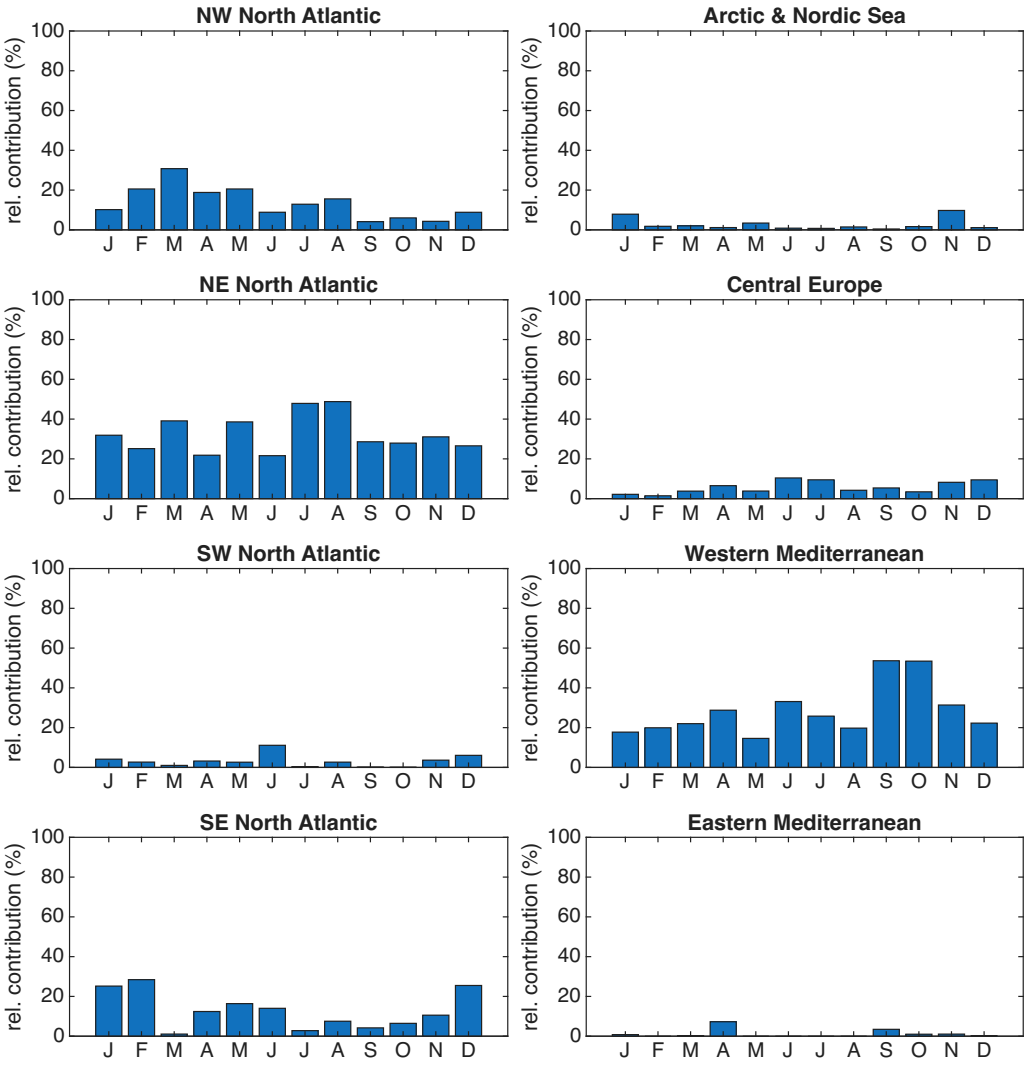

Figure C3: Relative contributions from the eight oceanic moisture source regions (% of final specific humidity).

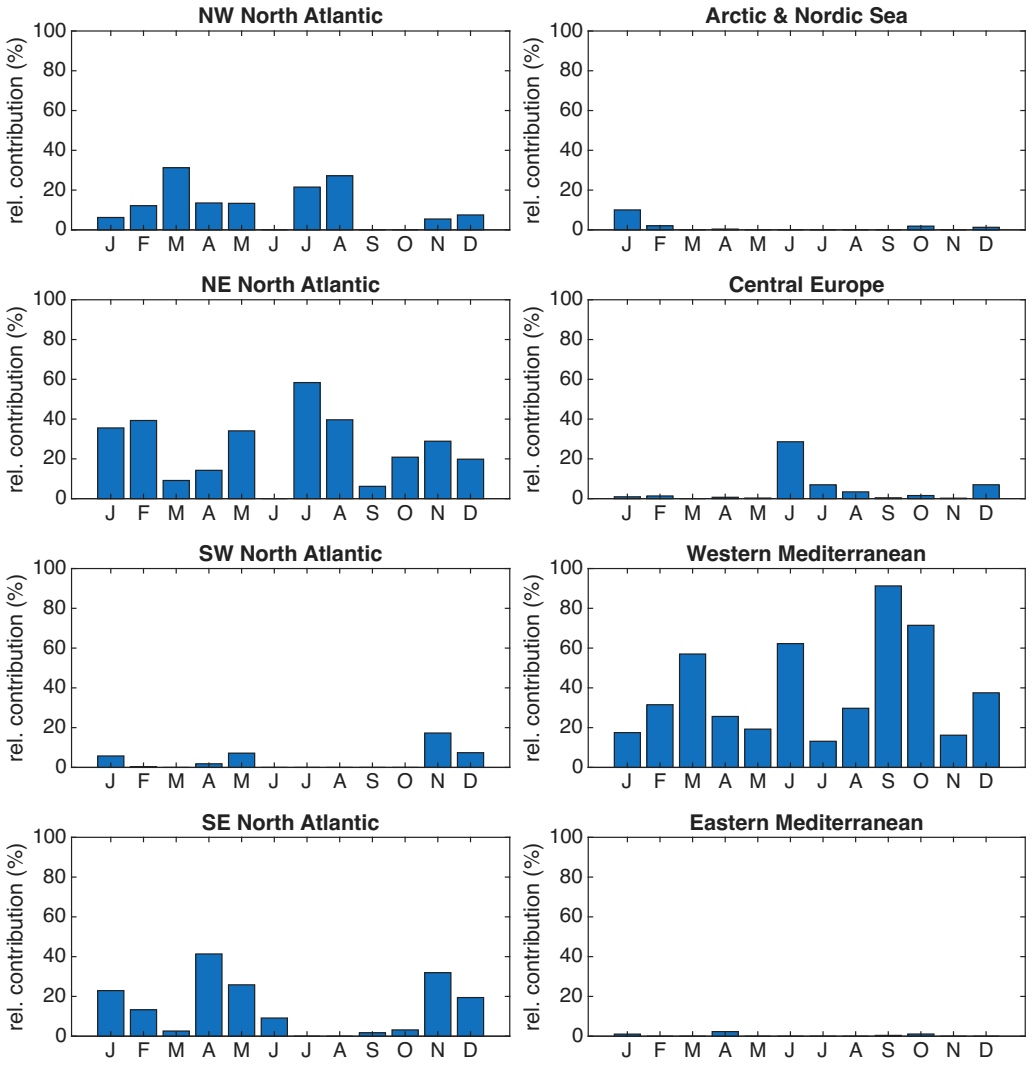

Figure C4: Relative contributions from the eight oceanic moisture source regions (% of accounted precipitation).

Table C1: Isotopic composition of atmospheric water vapor derived from the eight defined oceanic moisture source regions.

Moisture source region	$\delta^{18}O_V$ (‰)		d-excess$_V$ (‰)		^{17}O-excess$_V$ (per meg)		relative contribution to on-site moisture (%)
	AV	SD	AV	SD	AV	SD	
NW North Atlantic	-15.8	4.9	11.8	4.1	26	10	13
NE North Atlantic	-15.5	4.9	11.0	3.8	25	9	33
SW North Atlantic	-14.8	3.7	10.9	2.9	27	9	3
SE North Atlantic	-14.9	6.1	9.4	3.9	27	11	12
Arctic and Nordic Sea	-16.3	8.5	10.8	6.4	25	15	2
Central Europe	-17.7	5.0	12.9	4.0	26	9	6
Western Mediterranean	-14.8	4.9	11.2	3.6	26	9	29
Eastern Mediterranean	-16.6	4.7	13.2	4.7	34	12	1

Table C2: Isotopic composition of precipitation derived from the eight defined oceanic moisture source regions.

Moisture source region	$\delta^{18}O_P$ (‰)		d-excess$_P$ (‰)		^{17}O-excess$_P$ (per meg)		relative contribution to accounted P amount (%)
	AV	SD	AV	SD	AV	SD	

NW North Atlantic	-8.2	2.8	13.5	3.8	31	11	8
NE North Atlantic	-9.2	4.5	11.8	3.8	33	14	25
SW North Atlantic	-8.5	2.3	11.9	2.4	32	4	4
SE North Atlantic	-8.4	2.4	12.0	3.5	32	5	18
Arctic and Nordic Sea	-12.1	6.7	12.9	2.7	42	17	2
Central Europe	-7.5	4.3	10.3	7.9	28	14	2
Western Mediterranean	-7.6	2.9	11.9	3.8	29	7	41
Eastern Mediterranean	-10.0	8.4	11.2	10.1	34	25	1

Reviewer Comment:

- Abstract L20: Please clarify whether the authors refer to evaporation or evapotranspiration.

Author response:

We revised the abstract. This sentence has been removed.

Reviewer Comment:

- L104-115: I believe three mixing ratio sensitivity experiments are sufficient, assuming no change in the experimental setup during the study period. Please also report how may calibrations were performed (daily, weekly, etc). Was the water vapor Picarro also calibrated for the mixing ratio?

Author response:

Indeed, we analysed liquid standards weekly at four water mixing ratios (3000, 7000, 11000 and 17000 ppmv). As the results were consistent with the mean of the more highly resolved water mixing ratio functions, we neglected the measurements at 3000, 7000 and 17000 ppmv, used only the measurements at 11000 ppmv for calibration and the mean functions for mixing ratio dependency correction. We specify this now in the revised version.

Changes in the manuscript:

We detailed the corresponding paragraph in the methods section.

New Line 118-146:

The calibration protocol of atmospheric water vapor isotopic data is described in detail in Voigt et al. (2023). Three liquid water standards that covered the expected isotopic range of atmospheric water vapor at the study site were analyzed weekly using an autosampler system (A0325, Picarro Inc., California, USA) coupled to the high-precision vaporizer and the analyzer (Fig. 1). The liquid standards were injected in a dry air stream, produced by a lubricated mobile air compressor (MONTECARLO FC2, ABAC air compressors, Italy) and further dried using two drierite columns and a dry ice trap. Using dry ambient air instead of synthetic air as carrier gas for calibration of atmospheric water vapor isotope measurements is crucial to avoid any potential matrix effect (Voigt et al., 2022). From January to May, standards were analyzed at four water mixing ratios (3000 ppmv, 7000 ppmv, 11000 ppmv and 17000 ppmv) to assess temporal variability of the mixing ratio dependency. As no significant variation

was observed, measurements from June to November were conducted only at 11000 ppmv for VSMOW-SLAP normalization. The mixing ratio dependency functions for the three liquid standards were determined based on three higher-resolved water mixing ratio dependency assessments performed in May 2021, October 2021 and January 2022. From the end of November to December, standards were additionally analyzed at 5000 ppmv as atmospheric water mixing ratios were low. For details on the run architectures see Table A1.

For calibration, raw $\delta^{17}O$, $\delta^{18}O$ and $\delta^{2}H$ of the liquid standards from four consecutive runs (four weeks) were averaged and subsequently corrected to the water mixing ratio of the measured atmospheric water vapor:

$$\delta_{\mathrm{std,corr}} = \delta_{\mathrm{std,meas}} + a\left(\frac{1}{H_2O_{\mathrm{atm}}} - \frac{1}{H_2O_{\mathrm{std}}}\right) + b(H_2O_{\mathrm{atm}} - H_2O_{\mathrm{std}}) + c \qquad (1)$$

where δ denotes $\delta^{17}O$, $\delta^{18}O$ or $\delta^{2}H$ (in ‰), and H_2O is the measured water mixing ratio (in ppmv) of the standard (std) and the atmosphere (atm), respectively. The coefficients a, b and c describe the mixing ratio dependency functions and are specific for $\delta^{17}O$, $\delta^{18}O$ and $\delta^{2}H$ and for each standard (Table A2). The mixing ratio corrected values of the standards with the lowest and the highest isotopic values were then used for two-point calibration on VSMOW-SLAP scale, while the third standard with an intermediate isotopic composition served as quality control.

The precision of raw isotopic data was estimated from Allan deviation analysis of 24-hour in-situ measurements of atmospheric water vapor at O_3HP in June 2021. While the optimal integration time for $\delta^{17}O$, $\delta^{18}O$, $\delta^{2}H$ and d-excess is on the order of a few minutes, the Allan deviation of ^{17}O-excess reaches a minimum (~7 per meg) at an averaging time of about 1 hour (Fig. A1). To assess the precision of calibrated data, a Monte Carlo simulation was applied following Voigt et al. (2022). In 100 000 iterations, random normally distributed values were generated accounting for the standard deviations of (i) raw $\delta^{18}O_V$, $\delta^{2}H_V$ and $^{17}O\text{-excess}_V$, (ii) the coefficients of the mixing ratio dependency functions of each standard (Table A2) and (iii-iv) the measured and reference values of $\delta^{18}O$, $\delta^{2}H$ and ^{17}O-excess of the two standards. In each iteration, raw atmospheric values were calibrated following the above-described procedure.

We added the run architecture used for calibration in the appendix:

Table A1: Run architectures used for calibrations of atmospheric water vapor measurements.

Working standard	Number of injections	Water mixing ratio (ppmv)	Purpose	Data processing
JAN – MAY 2021				
ICE	20	22000	Conditioning	discard
ICE	10	17000	Validation of mixing ratio dependency function	discard first 5, average last 5
ICE	10	11000	Validation of mixing ratio dependency function, VSMOW-SLAP calibration	discard first 5, average last 5
ICE	10	6000	Validation of mixing ratio dependency function	discard first 5, average last 5

ICE	10	3500	Validation of mixing ratio dependency function	discard first 5, average last 5
NOC	10	22000	conditioning	discard first 5, average last 5
NOC	10	17000	Validation of mixing ratio dependency function	discard first 5, average last 5
NOC	10	11000	Validation of mixing ratio dependency function, VSMOW-SLAP calibration	discard first 5, average last 5
NOC	10	6000	Validation of mixing ratio dependency function	discard first 5, average last 5
NOC	10	3500	Validation of mixing ratio dependency function	discard first 5, average last 5
TAP	10	22000	Conditioning	discard first 5, average last 5
TAP	10	17000	Validation of mixing ratio dependency function	discard first 5, average last 5
TAP	10	11000	Validation of mixing ratio dependency function, VSMOW-SLAP calibration	discard first 5, average last 5
TAP	10	6000	Validation of mixing ratio dependency function	discard first 5, average last 5
TAP	10	3500	Validation of mixing ratio dependency function	discard first 5, average last 5
JUN – OCT 2021				
ICE	20	28000	Conditioning	discard
ICE	8	11000	VSMOW-SLAP calibration	discard first 2, average last 6
NOC	15	28000	Conditioning	discard
NOC	8	11000	VSMOW-SLAP calibration	discard first 2, average last 6
TAP	15	28000	Conditioning	discard
TAP	8	11000	VSMOW-SLAP calibration	discard first 2, average last 6
NOV – DEC 2021				
ICE	20	28000	Conditioning	discard
ICE	8	11000	Validation of mixing ratio dependency function, VSMOW-SLAP calibration	discard first 2, average last 6
ICE	8	5000	Validation of mixing ratio dependency function	discard first 2, average last 6
NOC	15	28000	Conditioning	discard
NOC	8	11000	Validation of mixing ratio dependency function, VSMOW-SLAP calibration	discard first 2, average last 6
NOC	8	5000	Validation of mixing ratio dependency function	discard first 2, average last 6
TAP	15	28000	Conditioning	discard
TAP	8	11000	Validation of mixing ratio dependency function, VSMOW-SLAP calibration	discard first 2, average last 6
TAP	8	5000	Validation of mixing ratio dependency function	discard first 2, average last 6

Reviewer Comment:

- L168-169: The sentence is unclear as currently written. Please rephrase.

Author response:

With the implementation of the quantative moisture source analysis precipitation events are not classified anymore per moisture source region but rather moisture sources per precipitation sample has been quantified. The sentence has been removed in the revised version.

Reviewer Comment:

- I suggest framing the geographical location of the study area more clearly in the context of the Mediterranean basin and the Atlantic Ocean. This information is currently discussed later in the manuscript (see Fig. 4), but it would be helpful to introduce it earlier, together with the description of the study site. It would be nice to have a single Figure showing the geographical location of the study area and a photo of the study site. Given that surrounding vegetation and landscape seem to be important actors in isotope processes at the ecosystem scale, visual context would be valuable. More on this, I have googled the coordinates and the observatory seems to be on a mountain slope. Do the authors expect wind direction or local circulation (e.g. mountain–valley breeze systems) to influence local moisture sources or boundary-layer dynamics?

Author response:

The region exhibits geological folding characteristic of the Alpine orogeny. The observatory is situated on a 15 km² raft foundation inclined at 2–4%, a configuration typical of the broader surroundings rather than a discrete topographic peak or ridge. Thermal turbulence and updraft manifesting is anticipated but uniformly distributed across the surrounding >20 km radius. While valleys may exhibit marginally elevated humidity episodically, open water bodies are negligible—limited to ephemeral streamlets—owing to the karstic limestone lithology, which facilitates rapid infiltration; most streamlets desiccate promptly post-precipitation. We will add a map with the study location and a photo from the study site.

Changes in the manuscript:

See new Fig. 1 in reply to Major Comment #2.

Reviewer Comment:

- A schematic representing the measurement setup is missing. A simple diagram illustrating the measurement setup would greatly improve clarity.

Author response:

A figure representing the measurement setup is provided in the revised version.

Changes in the manuscript:

See new Fig. 1 in reply to Major Comment #2.

Reviewer Comment:

- Modeling the isotopic evaporation flux (L180): if the authors refer to the exponent n controlling the ratio of water vapor isotopolues diffusivities in air (see, e.g eq. 17 in Horita et al., 2008) it should be noted several works show smaller effective values of n, following e.g. Duetsch et al. (2025, Figure 2) and experimental evidences in references therein.

Author response:

The turbulence coefficient is an empirical parameter that cannot be directly measured. We adjusted the turbulence coefficent to roughly fit d-excess data. A value of 0.33 was adopted, which is at the upper end of previously reported values. Using lower values implies lower kinetic fractionation during evaporation and thus lead to lower d-excess and ^{17}O-excess values in the resulting water vapor. We now detail this in the revised version.

Changes in the manuscript:

New Line 245-251:

The turbulence coefficient is an empirical parameter that quantifies the contribution of molecular diffusion to the total kinetic fractionation during evaporation. Several studies have attempted to constrain this parameter empirically (e.g., Pfahl and Wernli, 2008; Uemura et al., 2010; Zannoni et al., 2022) and to develop theoretical frameworks (Horita et al., 2008; Xia et al. 2023; Duetsch et al., 2025). The turbulence coefficient has been adjusted to 0.33, which is at the upper end of previously reported values for open-ocean evaporation (see, e.g., Gat, 1996; Pfahl & Wernli, 2008; Uemura et al., 2010, Duetsch et al., 2025). Lower turbulence coefficients correspond to lower kinetic fractionation during evaporation and therefore lower d-excess and 17O-excess values in the evaporated water vapor.

Reviewer Comment:

- Figure 1 c: evidence of fractionated precipitation during summertime (negative d-excess)

Author response:

Yes, this is an indication for re-evaporation of the precipitation during falling as analysed in detail in Section 3.4 and discussed in Section 4.1. No changes have been made in the revised manuscript.

Reviewer comment:

- L284: For δ18O and δD might be of interest of comparing with similar studies that were performed for long time-intervals in different climate settings such as Chen et al., 2024, Deshpande et al. 2010.

Author response:

We now set our results in isotopic equilibrium between precipitation and atmospheric water vapor on annual scale in the context with findings in other environmental settings.

Changes in the manuscript:

New Line 535-540:

At annual scale, the opposing winter and summer monthly $\Delta\delta^{18}O_{Veq\text{-}V}$ values at our study site effectively cancel each other out, so that $\delta^{18}O_{Veq}$ closely approximates $\delta^{18}O_V$ (cf., Voigt et al., 2023). However, this may differ depending on the environmental setting. Significant deviations from isotopic equilibrium at annual scale were observed in monsoonal areas due to rain re-evaporation (Desphande et al., 2010; Landais et al., 2010; Wen et al., 2010), convective activity (Risi et al., 2012; Tremoy et al., 2014; Xia et al., 2022) or in environments with seasonal precipitation, where the isotopic composition of precipitation is not representative for annual average atmospheric water vapor (Tsujimura et al., 2007; Voigt et al., 2021).

Reviewer Comment:

- Figure 4: The caption length should be reduced and discussion of the results should be moved from the caption to the main text (sect. 3.4)

Author response:

We reduced the length of the caption. The removed information was already provided in the discussion so that we did not change the main text.

Changes in the manuscript:

Figure 5: Isotope difference (Δ) between water vapor estimated from isotope equilibrium with precipitation (V_{eq}) and amount-weighted atmospheric water vapor measured at 12.5 m above ground level (V) for each precipitation event in 2021. Data is coloured according to season. The blue-shaded area indicates samples for which the equilibration between precipitation and near-surface atmospheric water vapor is likely incomplete. Precipitation samples that correspond to data falling within the grey-shaded area are likely affected by re-evaporation during fall through the air column.

Reviewer Comment:

- L342-346: The discussion of NAO phases and water vapor isotope composition is interesting but only briefly mentioned. It is worth noting that other studies identified strong links between NAO phases, weather regimes and ground-level water vapor and precipitation isotope composition e.g.: Deininger et al. (2016) for precipitation over continental Europe in winter, Zannoni et al. (2019) for water vapor at ground level in the Mediterranean basin. A short expansion or contextualization would strengthen this section.

Author response:

We provide now some context to the analysis of weather regimes in the methods and add a separate section on the weather regimes in the discussion.

Changes in the manuscript:

New line 190-196:

Synoptic atmospheric variability over Europe can be characterized using weather regimes (Cassou, 2008; Cassou et al., 2005; Michelangeli et al., 1995; Vautard, 1990). Previous studies have demonstrated strong positive correlations between $\delta^{18}O_P$ and $\delta^{2}H_P$ and the NAO index (Baldini et al., 2008; Field, 2010; Deininger et al., 2016; Zannoni et al., 2019). In addition, Zannoni et al. (2019) reported a negative correlation between both d-excess$_V$ and d-excess$_P$ and the NAO index at a coastal lagoon in Venice. These correlations are strongest in central Europe but are often weaker in mountainous and circum-Mediterranean regions, where local orographic effects and moisture recycling modify the isotopic composition of precipitation (Baldini et al., 2008).

New Line 541-549:

4.6 Effect of the weather regimes

The absence of correlation between the weather regimes and the isotopic composition of vapor and precipitation is probably due to the combined influence of multiple moisture sources weakly isotopically contrasted as presented in Section 3.6. In addition, local moisture recycling may further modify the isotopic signal of atmospheric water vapor and, thus, precipitation, as previously suggested for the circum-Mediterranean region (Baldini et al., 2008). It is also possible that the isotopic composition of near-surface atmospheric water vapor differs slightly from that at the precipitation formation height due to ground roughness, convection, mixing processes in the planetary boundary layer (Griffis et al., 2016; Salmon et al., 2019; Tada et al., 2021).

Reviewer Comment:

- L346-347: Water vapor isotopic composition measured near the surface can be representative of the boundary layer, but its variability may be modulated by ground roughness/homogeneity, convection, mixing, climate and weather regime, time of the day among the most important. Aircraft and tall-tower measurements provide strong evidence in this regard: see e.g. Salmon et al. (2019), Griffis et al. (2016)

Author response:

We thank the reviewer for this clarification. We have implemented this information in the discussion. See reply to previous comment.

Reviewer Comment:

- L391-394, L407-409, Figure 5.i: what the 17O-excess composition of the seawater source should be to agree with observed atmospheric water vapor value?

Author response:

As specified in the Sect. 4, the isotopic composition of the source water of evaporation influences the isotopic composition of the evaporated water vapor. If the seawater would have

5 instead of the assumed -5 per meg, the ^{17}O-excess of the evaporated water vapor would be 10 per meg higher.

Reviewer Comment:

- L427: compounded forms such as "kppmv" are not recommended under metrology standards. Just reports "thousands of ppmv" or simply "< 4000 ppmv"

Author response:

We thank the reviewer for clarification. This has been changed in the revised version

Reviewer Comment:

- L428-430: Rayleigh distillation assumes isotopic equilibrium. These conditions are applicable inside a cloud (100% RH), but not for most of the conditions reported in this study.

Author response:

This part has been removed as part of the revisions.

Author responses to Reviewer #2

Reviewer Comment:

1. The interpretation of the diurnal isotopic variability neglects the influence of vertical mixing within the PBL that has been identified in many previous studies of d18O, dD, and deuterium-excess. See Griffis et al., 2016 and references therein. It is reasonable to believe that this process is also a major influence on 17O-excess.

2. Additionally, the influence of nighttime water exchange between the surface and the atmosphere does not have to be confined to leaf waters. Soil water vapor exchange may also play a role as noted by Berkelhammer et al. 2013.

Author response:

We agree that entrainment of the residual layer, a remnant of the convective boundary layer that developed during the previous day, can contribute to increasing ^{17}O-excess and d-excess as suggested in previous studies. However, we think that entrainment from the free troposphere is unlikely to have a significant influence due to its low water content. We also agree that water exchange between the atmosphere and highly evaporated surface soil layers can also contribute to lowering of ^{17}O-excess$_V$ and d-excess$_V$ during night. We note that late afternoon leaf waters are usually more depleted than soil waters at our study site so that even low exchange rates can have a significant impact.

Changes in the manuscript:

We have entirely revised the discussion on the influence of terrestrial moisture recycling on atmospheric water vapor and implemented the discussion points raised by the reviewer.

New Line 474-5497:

On a daily scale, χ, d-excess$_V$ and ^{17}O-excess$_V$ are higher and d^{18}O$_V$ is lower during the day (with a peak in the afternoon) than at night. Such a day-night pattern has been reported for d-excess$_V$ across diverse environments, including forests, grasslands, wetlands, agricultural areas and urban regions (Berkelhammer et al., 2013; Delattre et al., 2015; Welp et al., 2012) and attributed to several processes, including entrainment of the residual layer or air from the lower free troposphere in the boundary layer (Lai & Ehleringer, 2011; Simonin et al., 2014), local evapotranspiration fluxes (Huang & Wen, 2014; Simonin et al., 2014; Welp et al., 2012; Zhao et al., 2014; Delattre et al., 2015), and dewfall evaporation (Bastrikov et al., 2014; Berkelhammer et al., 2013). The fact that the observed day-night pattern in d-excess$_V$ and ^{17}O-excess$_V$ is more pronounced during the forest growth period and most pronounced near surface (Fig. 4) supports the key influence of surface-atmosphere processes. Assuming that the soil water has an isotopic composition close to that of precipitation, soil water evaporation decreases d^{18}O$_V$ and increases d-excess$_V$ and ^{17}O-excess during the day (Craig & Gordon, 1965; Rothfuss et al., 2021; Fig. 7). Plant transpiration, which is assumed to be non-fractionating relative to soil water (Galewsky et al., 2016 and references therein) increases d^{18}O$_V$ but has little impact on d-excess$_V$ and ^{17}O-excess$_V$ (Fig. 7). In total, net evapotranspiration affects d^{18}O$_V$, with the direction and magnitude depending on the relative contributions of evaporation and transpiration, whereas d-excess$_V$ and ^{17}O-excess$_V$ are elevated only when evaporation is substantial (Fig. 7). Entrainment of a remnant of the convective boundary layer of the previous day, with a high d-excess$_V$ and ^{17}O-excess$_V$ used by evapotranspiration, may amplify the increase in d-excess$_V$ and ^{17}O-excess$_V$ in the morning (Lai & Ehleringer, 2011; Simonin et al., 2014,Griffis et al. 2016; Welp et al., 2012). Entrainment of the lower free troposphere may also occur. However, the low water vapor mixing ratio of the free troposphere (< 4000 ppmv) likely limits its influence on the isotopic composition of atmospheric water vapor. During the night, when RH is high, water exchange between plant water subjected to incomplete stomata closure, or evaporated surface soil waters, and the atmospheric water vapor can increase d^{18}O$_V$ and decrease d-excess$_V$ (Berkelhammer et al., 2013; Bastrikov et al., 2014; Lai & Ehleringer, 2011; Simonin et al., 2014; Welp et al., 2012) and ^{17}O-excess$_V$. The combination of all these factors likely contributes to the observed day-night pattern in d^{18}O$_V$, d-excess$_V$ and ^{17}O-excess$_V$. On the monthly scale, these day-night vegetation-related isotopic variations cancel each other out. This contradicts the previously proposed hypothesis that continental evaporation masks the correlation between NAO and δ^{18}O$_P$ in the circum-Mediterranean area (Baldini et al. 2008).

Reviewer Comment:

3. In the conclusions, it's stated that 17O-excess can separate evaporation and transpiration signals. D-excess has this potential too, but neither is shown in this dataset. Please provide support or remove that conclusion.

Author response:

Indeed, our results do not directly show that ^{17}O-excess can separate evaporation and transpiration signals. Instead, we show that it is helpful to identify the contribution of evapotranspiration to the atmosphere on local scale. The magnitude of change in ^{17}O-excess together with changes in the atmospheric water mixing ratio potentially allows quantification of its impact, but this is beyond the scope of this study.

Changes in the manuscript:

The conclusions have been revised to implement the kewly integrated key messages. Regarding the moisture recycling, the conclusion reads as follows now:

New Line 588-596:

On the diurnal scale, our results demonstrate that ^{17}O-excess$_V$ exhibits a similar diurnal pattern as observed previously for d-excess$_V$ in different environmental settings. Increases in ^{17}O-excess$_V$ and d-excess$_V$ during daytime likely reflect the combination of vegetation-related processes, including soil water and dewfall evaporation, plant transpiration and entrainment of a remnant of the convective boundary layer of the previous day. Nighttime decreases in both tracers likely result from continued isotopic exchange between leaf water, evaporated surface soil water, and ambient water vapor. These findings highlight the strong control of local evapotranspiration processes on sub-daily variability of ^{17}O-excess$_V$ and d-excess$_V$. However, such effects are not evident in monthly ^{17}O-excess$_V$ and d-excess$_V$ as opposing day- and nighttime contributions largely offset each other at the daily scale. This study opens new avenues for investigating land-atmosphere water exchange across diverse climates, vegetation types and timescales.

Reviewer Comment:

4. Please provide more description of how uncertainty in 17O-excess and deuterium-excess are quantified. See specific comments below.

Author response:

This comment was also raised by Reviewer #1. A more detailed description is now provided. For details, please see author response to Reviewer #1 above.

Reviewer Comment:

5. As reviewer #1 mentions, the moisture source region discussion is rather qualitative, and I agree with many of their points.

Author response:

We have implemented a quantitative Lagrangian moisture source analysis and combined it with a Weighted Trajectory apporach of Salamalikis et al (2015). For details, please see author response to Reviewer #1 above.

Reviewer Comment:

Section 2.1: Include canopy LAI, tree stem density, or other metric of closed vs. open canopy so that vertical mixing with the boundary layer can be put into context.

Author response:

This information is provided in the revised version.

Changes in the manuscript:

New Line 74-76:

In 2021, the stand density was about 3550 trees per hectare with a stand basal area 18.8 m^2 ha^{-1}, an average leaf area index of about 2 m^2 m^{-2}, ranging between 1 and 3 m^2 m^{-2}, and a canopy gap fraction of about 25% (LAI-2000, LI-COR Inc., Nebraska, USA).

Reviewer Comment:

Line 37: unclear meaning: 'recharge conditions during lake evaporation (Surma et al., 2015, 2018)'

Author response:

The phrase has been revised.

Changes in the manuscript:

New Line 37-41:

Moreover, the ^{17}O-excess of surface waters can be used for identifying if a lake receives continuous surface or subsurface inflow (Surma et al., 2015, 2018), mixing processes between evaporated and unevaporated waters (Voigt et al., 2021), quantifying lake hydrological balance (Pierchala et al., 2021; Voigt et al., 2024) and tracing water exchange at the soil-plant-atmosphere interface (Landais et al., 2006; Li et al., 2017; Voigt et al., 2023).

Reviewer Comment:

Line 66: Do these site acronyms mean anything? ‘AnaEE in natural experimental platform O3HP’

Author response:

These acronyms are specified in the revised version.

Changes in the manuscript:

New Line 69-71:

The AnaEE (European Research Infrastructure 'Analyses and Experimentation on Ecosystems') *in natura* facility O_3HP (Oak Observatory of the Upper-Provence Observatory) is situated in a deciduous Mediterranean forest about 70 km inland, north of Marseille (France) at an altitude of 680 m above sea level (43.935° N, 5.711° E, Fig. 1a).

Reviewer Comment:

Section 2.2: 5 L/min continuous flushing of inlet lines with 70 min switching is likely sufficient for d18O and dD, but I’m not familiar with typical memory timescales for 17O-excess. While I don’t expect d17O memory to be longer than d18O, a demonstration of step-change response curves or discussion of equilibration time for this system would be appreciated.

Author response:

As memory effects for oxygen are generally lower than for δ^2H and as similar memory effects have been found for $\delta^{17}O$ and $\delta^{18}O$ in liquid measurements so that ^7O-excess is not affected (Vallet-Coulomb et al., 2021). In addition, lines were flushed with 5 L/min and the first 10 min of each line measurement were removed. Therefore, we believe that impact of the memory effect on our measurements is minimal. In the initial author response we show results to assess the memory effect. Please see there for details. No changes were made in the revised version.

Reviewer Comment:

Line 115: ‘Precision was better than 0.1 ‰, 0.2 ‰, 1.8 ‰ and 14 per meg, and 0.9 ‰ for δ17O, δ18O, δ2H, 17O-excess, and d-excess, respectively.’ How was precision quantified? Averaging over a defined time period? Propagation of error of d18O and dD would result in a d-excess uncertainty of 3.4 permil, much greater than the authors’ estimate of 0.9 permil.

Author response:

Details on the assessment of precision of calibration atmospheric water vapor isotope data are now provided. See response to reviewer’s major comment 4 above.

Reviewer Comment:

Line 191: ‘The average wind speed at 10 m height was 0.3 m s-1’ How is the stdev determined?

Author response:

We now provide the standard deviation over the daily average wind speed, which is 1.1 m s^{-1}.

Reviewer Comment:

Line 195: 'The largest day-night differences occurred near the ground and in summer (Fig. A1-A3). During the day, q and Tair were highest near the ground, whereas RH was vertically homogenous (Fig. A1-A3). At night, the Tair vertical gradient was inverted, with the lowest values occurring near the ground, while q showed no vertical variation, resulting in decreasing RH from the surface to 10 m agl (Fig. A1-A3).' Assuming this refers to summer conditions, wouldn't it be unusual for air temp to be cooler near the surface than above when the surface usually radiates heat at night?

Author response:

Nighttime gradients in T and q are rather weakened (Fig. B1-B3). Overall cooling leads to higher RH compared to daytime that decrease from ground to 10 m agl. The section has been rephrased in the revised version (see reply to Reviewers major comment 1 & 2).

Reviewer Comment:

Section 3.6: what frequency of observations was this analysis based on? Monthly means or hourly resolution?

Author response:

This analysis is based on the moisture source identification using the hourly air-mass back trajectory analysis.

Reviewer Comment:

Fig 6: 17O-excessv is different for summer and winter. Driven by RHsst differences. The process label 'E' is not described in the text.

Author response:

E refers to evaporation from open-surface waters or soil, while T is plant transpiration. We specify this now in the revised version.

Reviewer Comment:

Section 4.1: These patterns are consistent with many other continuous water vapor isotope studies including d-excess and citations should be included. The novelty here is adding on 17O-

excess and comparing how it's similar/different from d-excess as it's sensitive to many of the same influences.

Author response:

We revised Section 4.1and the conclusion section to better highlight the novelty of ^{17}O-excess and compare magnitudes for d-excess and 17O-excess.

Reviewer Comment:

Line 371: 'thus the isotope compositions of water vapor evaporated from these sources are ***predicted to be*** similar.' I suggest qualifying this statement because later the authors mention uncertainty in the inputs for calculating these estimates.

Author response:

We have revised this phrase as suggested.

Reviewer Comment:

Line 420-430: could use improved citations and is misleading in present form. Berkelhammer et al., 2013 and references therein attribute diurnal variability to increased vertical mixing or PBL entrainment during the daytime as well as vapor exchange with the surface (leaf water and soil water) at night. The authors minimize this process because PBL air is drier, but nevertheless, it has been previously shown to be important and is likely contributing here also. Some well-documented entrainment influence citations like Griffis et al., 2016 and Welp et al., 2012 should be included.

Author response:

This was major point #1 of reviewer #2. See author response above.

Reviewer Comment:

Line 430: The authors argue that Rayleigh distillation is not expected to lead to 17O-excess enrichment in the lower free troposphere. Xia et al., 2023 shows theoretical deuterium-excess and 17O-excess signals increase as Rayleigh distillation intensifies.

Author response:

According to Fig. 3 in Xia et al. (2023) the ^{17}O-excess of atmospheric water vapor is increasing not more than 5 per meg considering only liquid condensation (Fig. 3b) and can even decrease by more than 30 per meg when condensation has ice (Fig. 3d). Thus, a ^{17}O-excess$_V$ in the lower troposphere is expected to be similar or even lower than near ground. We have added the citation of Xia et al. (2023) in the revised version.

Reviewer Comment:

Line 440-443: Ice/snow formation in cloud is likely not in isotopic equilibrium with cloud vapor due to super saturation effects Dutsch et al., 2019 and Xia et al., 2023.

Author response:

We thank the reviewer for noting this. We now specify the difference in isotope fractionation for liquid and solid precipitation.

Changes in the revised manuscript:

New Line 508-512:

Liquid precipitation forms in isotopic equilibrium with atmospheric water vapor at cloud height, while ice formation may be accompanied by an additional kinetic effect due to supersaturation of water vapor (Dütsch et al., 2017, Xia et al., 2023). Vapor at cloud height is typically depleted in heavy isotopes compared to near-surface atmospheric water vapor due to Rayleigh fractionation processes (Giménez et al., 2021 and references therein; Salmon et al., 2019; Sodemann et al., 2017).

Reviewer Comment:

Line 467: main conclusions are mostly asserted by theory rather than using observations as an independent test.

Author response:

The conclusions have been revised to better highlight key findings of the present study and remaining challenges.

Changes in the manuscript:

New Line 567-609:

This study provides a unique dataset of the triple oxygen and hydrogen isotopic composition of atmospheric water vapor and precipitation in a Mediterranean oak forest ecosystem, highlighting seasonal and diurnal variability and their underlying drivers. Our findings demonstrate the strong potential of ^{17}O-excess as a complementary tracer for disentangling fractionation processes and providing complementary hydrological insights.

The Western Mediterranean, The NE North Atlantic and the SE North Atlantic are identified as the principal moisture sources for vapor and precipitation at the study site. Theoretically predicted seasonal variations in d-excess$_V$ and ^{17}O-excess$_V$ over these oceanic moisture sources, driven by changes in RH_{SST}, are preserved in the atmospheric water vapor observed at the study site. In contrast, $d^{18}O_V$ is only weakly influenced by source conditions and mainly reflects Rayleigh distillation during air mass transport. Monthly values of $d^{18}O_P$, d-excess$_P$ and ^{17}O-excess$_P$ show a similar seasonal pattern to atmospheric water vapor but are modified in summer due to sub-cloud rain re-evaporation.

Despite these source-related controls on d-excess$_V$ and ^{17}O-excess$_V$, neither tracer clearly discriminates oceanic moisture source regions or weather regimes at monthly scale, likely due to weak isotopic contrasts between the oceanic moisture sources and frequent mixing of moisture from multiple sources. This result contrasts with previous studies that attributed higher d-excess$_P$ from Western Mediterranean sources compared to the North Atlantic sources to enhanced kinetic fractionation during evaporation, driven by lower RH_{SST} (Casellas et al., 2019; Celle-Jeanton et al., 2001; Cruz-San Julian et al., 1992; Delattre et al., 2015; Natali et al., 2021). On the other hand, we do observe lower $\delta^{18}O_P$ from North Atlantic sources compared to the Western Mediterranean sources, consistent with earlier observations (Casellas et al., 2019; Celle-Jeanton et al., 2001; Cruz-San Julian et al., 1992; Delattre et al., 2015; Natali et al., 2021). This difference is likely related to enhanced rainout along the longer air mass transport pathway from the North Atlantic. Overall, these findings imply that long-term precipitation isotopic records of precipitation preserved in Mediterranean continental paleoclimate archives should be interpreted with caution when inferring shifts in moisture source regions.

On the diurnal scale, our results demonstrate that ^{17}O-excess$_V$ exhibits a similar diurnal pattern as observed previously for d-excess$_V$ in different environmental settings. Increases in ^{17}O-excess$_V$ and d-excess$_V$ during daytime likely reflect the combination of vegetation-related processes, including soil water and dewfall evaporation, plant transpiration and entrainment of a remnant of the convective boundary layer of the previous day. Nighttime decreases in both tracers likely result from continued isotopic exchange between leaf water, evaporated surface soil water, and ambient water vapor. These findings highlight the strong control of local evapotranspiration processes on sub-daily variability of ^{17}O-excess$_V$ and d-excess$_V$. However, such effects are not evident in monthly ^{17}O-excess$_V$ and d-excess$_V$ as opposing day- and nighttime contributions largely offset each other at the daily scale. This study opens new avenues for investigating land-atmosphere water exchange across diverse climates, vegetation types and timescales.

At the process scale, summer precipitation shows strong coupling between $\delta^{18}O_P$, ^{17}O-excess$_P$ and d-excess$_P$, indicating rain re-evaporation. In contrast, negative $\Delta\delta^{18}O_{V_{eq}-V}$ values in winter suggest incomplete isotopic equilibration with ambient vapor. Although precipitation often deviates from isotopic equilibrium with near-surface atmospheric water vapor at the event scale, equilibrium water vapor reliably approximates the near-surface isotopic composition of atmospheric water vapor at monthly or annual scale. These findings have important consequences 1) for reconstructing the isotopic composition of atmospheric water vapor to constrain hydrological models of evaporative fractionation when direct measurements are not available, and 2) for simulating the isotopic composition of precipitation in isotope-enabled climate models. Our results support the robustness of reconstructions assuming isotopic equilibrium at annual scales in this climate context. However, at daily- to event scales, accurate reconstruction of the isotopic composition of atmospheric water vapor and simulation of rainfall formation require accounting for post-condensation processes, such as raindrop re-evaporation and rain-vapor equilibration during raindrop fall through the atmospheric column. When process scale dynamics are targeted, simultaneous measurements of triple oxygen and

hydrogen isotopes in precipitation and atmospheric water vapor are essential across diverse environmental settings to further constrain and improve the representation of these processes in isotope-enabled models.

Reviewer Comment:

Line 473: The findings in this paper contrast previous findings that mediterranean moisture source has a high deuterium-excess compared to North Atlantic, both in theoretical predictions and observations of downwind vapor and precipitation. What makes this study different? Different assumptions about conditions in the source regions? Perhaps ERA5 doesn't accurately capture near-surface RH differences? Does monthly resolution mute signal? Etc.

Author response:

High d-excess values in atmospheric water vapor and precipitation (> 20‰) are mainly observed in the Eastern Mediterranean (Casellas et al., 2019; Celle-Jeanton et al., 2001; Cruz-San Julian et al., 1992; Delattre et al., 2015; Natali et al., 2021). However, the Eastern Mediterranean contributes insignificant moisture to our study site. As we state in the manuscript, often multiple moisture sources contribute to specific humidity at our study so that the isotopic composition of atmospheric water vapor likely represents a mixed signal. Other factors such as local orographic effects or boundary layer dynamics can also diminish isotopic differences between moisture sources.

Changes in the manuscript:

Section 4.1 has been revised.

New Line 450-459:

In previous studies, evaporative conditions at the moisture sources were invoked to explain d-excess$_P$ in precipitation from the Western Mediterranean (~14 ‰) to be higher than in precipitation from the NE North Atlantic (~10 ‰) (Casellas et al., 2019; Celle-Jeanton et al., 2001; Cruz-San Julian et al., 1992; Delattre et al., 2015; Natali et al., 2021). Theoretical predictions indeed show that d-excess$_V$ over NE North Atlantic is about 3.7 ‰ lower than over Western Mediterranean due to higher RH_{SST} (Fig. 6). Similarly, ^{17}O-excess of water vapor evaporated from the Western Mediterranean is predicted to be ~ 6 per meg higher than from the NE North Atlantic, although the magnitude remains within measurement precision. However, d-excess and ^{17}O-excess measured in atmospheric water vapor and precipitation at O_3HP grouped by their primary moisture source (NE North Atlantic vs. Mediterranean) were not significantly different. Several factors may have contributed to diminish the isotopic contrast between these source regions, including frequent mixing of moisture from multiple sources, local orographic and boundary-layer dynamics or moisture recycling during atmospheric transport (Aemisegger et al., 2014; Natali et al., 2022).

Reviewer Comment:

Fig 2: d-excess deserves error bars also

Author response:

The error bars of d-excess are smaller than symbol size. This is now specified in the figure caption.

Reviewer Comment:

Fig 3: What frequency of data was used for the monthly means? 15-min or hourly, etc. Is the plot a smoothed spine fit through discrete values?

Author response:

We used hourly data to calculate monthly means. The curves show the discrete monthly mean values per hour of the day.

Reviewer Comment:

Fig A8: please include d-excess vs 17O-excess correlation here or somewhere in the paper

Fig A10: There are more statistics that could be helpful for the reader. The spread of back trajectories and/or the frequency of each cluster over the year.

Table B2: How is the SD of veq determined. The precip is collected monthly and event scale during some months, so are different methods used?

Author response:

The appendix has been restructured and additional figures and tables are provided in the revised version.